Excitatory Signaling in Bacteria Probed by Caged Chemoeffectors

Shahid Khan,* Fred Castellano,* John L. Spudich,‡ James A. McCray,§ Roger S. Goody,¶ Gordon P. Reid,‖ and David R. Trentham‖

*Department of Physiology and Biophysics, Albert Einstein College of Medicine, Bronx, New York 10461; ‡Department of Microbiology and Molecular Genetics, University of Texas, Medical School, Health Science Center, Houston, Texas 77030; §Department of Physics, Drexel University, Philadelphia, Pennsylvania 19104; ¶Max Planck Institut fur Medizinische Forschung, Abteilung Biophysik, Jahnstrasse 29. D6900 Heidelberg, Germany, and ‖National Institute for Medical Research, Mill Hill, London, NW7 1AA, UK

ABSTRACT Chemotactic excitation responses to caged ligand photorelease of rapidly swimming bacteria that reverse (*Vibrio alginolyticus*) or tumble (*Escherichia coli* and *Salmonella typhimurium*) have been measured by computer. Mutants were used to assess the effects of abnormal motility behavior upon signal processing times and test feasibility of kinetic analyses of the signaling pathway in intact bacteria. *N*-1-(2-Nitrophenyl)ethoxycarbonyl-L-serine and 2-hydroxyphenyl 1-(2-nitrophenyl) ethyl phosphate were synthesized. These compounds are a 'caged' serine and a 'caged' proton and on flash photolysis release serine and protons and attractant and repellent ligands, respectively, for Tsr, the serine receptor. The product quantum yield for serine was 0.65 (±0.05) and the rate of serine release was proportional to $[H^+]$ near-neutrality with a rate constant of 17 s^{-1} at pH 7.0 and 21°C. The product quantum yield for protons was calculated to be 0.095 on 308-nm irradiation but 0.29 (±0.02) on 300–350-nm irradiation, with proton release occurring at >10^5 s^{-1}. The pH jumps produced were estimated using pH indicators, the pH-dependent decay of the chromophoric *aci*-nitro intermediate and bioassays. Receptor deletion mutants did not respond to photorelease of the caged ligands. Population responses occurred without measurable latency. Response times increased with decreased stimulus strength. Physiological or genetic perturbation of motor rotation bias leading to increased tumbling reduced response sensitivity but did not affect response times. Exceptions were found. A CheR-CheB mutant strain had normal motility, but reduced response. A CheZ mutant had tumbly motility, reduced sensitivity, and increased response time to attractant, but a normal repellent response. These observations are consistent with current ideas that motor interactions with a single parameter, namely phosphorylated CheY protein, dictate motor response to both attractant and repellent stimuli. Inverse motility motor mutants with extreme rotation bias exhibited the greatest reduction in response sensitivity but, nevertheless, had normal attractant response times. This implies that control of CheY·phosphate concentration rather than motor reactions limits responses to attractants.

INTRODUCTION

Amino acid chemotaxis in the bacteria, *Escherichia coli* and *Salmonella typhimurium*, provides a particularly well understood example of sensory signal processing in single cells. The physiology of bacterial chemotaxis has been studied extensively (Berg, 1988), the gene loci coding for the proteins comprising the chemotactic machinery have all been identified (Parkinson and Kofoid, 1992), and much has been learned regarding the biochemistry of the protein-protein interactions and protein modification reactions (Bourret et al., 1991; Stock et al., 1991).

E. coli utilizes a battery of chemoreceptors to monitor its environment. The most abundant chemoreceptor, Tsr, senses the attractant amino acid serine and certain repellents, including protons. Binding of attractant to, or dissociation of repellent from Tsr signals counterclockwise (CCW) rotation of the locomotory organelles, the flagella. CCW signals enhance smooth-swimming runs. Binding of repellents, or dissociation of attractants, signals clockwise (CW) rotation. CW signals enhance cell tumbling or inverse swimming. Tsr-mediated chemotaxis involves six cytoplasmic proteins: CheA, CheB, CheR, CheW, CheY, and CheZ. Autophosphorylation of the histidine kinase, CheA, is modulated in vitro by chemoreceptor containing membrane preparations (Borkovich and Simon, 1992). CheA transfers phosphate in vitro to CheY and CheB. CheY·phosphate is dephosphorylated by CheZ (Bourret et al., 1991; Stock et al., 1991) Correlation between CheY·phosphate levels and flagellar motor CW/CCW rotation bias has been shown in semienvelope preparations (Barak and Eisenbach, 1992a). Adaptation to attractant addition, or repellent withdrawal, is mediated by methylation of multiple residues on the cytoplasmic domain of Tsr and analogous chemoreceptors by the methyltransferase, CheR. Adaptation to attractant withdrawal, or repellent addition, involves demethylation by the methylesterase, CheB (Spriager et al. 1979).

These observations are consistent with biochemical models (Gegner et al., 1992; Hess et al., 1988) whereby flagellar CW/CCW rotation bias follows changes in intracellular CheY·phosphate levels due to signals generated by ligand binding to receptor-CheW-CheA complexes, whereas control of CheA-CheB phosphotransfer provides adaptive feedback. A large number of chemotactic mutants have been isolated based on abnormal migration on agar swarm plates (Wolfe and Berg, 1989), in concentration gradients formed

Received for publication Received 8 June 1993 and in final form 1 September 1993.

Address reprint requests to Dr. Shahid Khan, Dept. of Physiology and Biophysics, Albert Einstein College of Medicine, Bronx, NY 10461.

0006-3495/93/12/2368/15 $2.00

at capillary tips (Adler, 1973), in density gradients stabilized against convection (Dahlquist et al. 1972, Weiss and Koshland, 1988), and across microchannel plates (Berg and Turner, 1990). An important achievement of chemotaxis models has been the ability to explain the abnormal swim-tumble balance of chemotactic mutants. Thus, CheB and CheZ null mutants have a tumbly phenotype, whereas CheA and CheY null mutants have a smooth-swim phenotype, as predicted by the models. Phosphorylation defective mutants generated by in vitro (Oosawa et al., 1988) and site-specific mutagenesis (Bourret et al., 1990; Lukat et al., 1991) also have a steady-state motile phenotype consistent with such models.

Bacteria respond to temporal rather than spatial gradients (Macnab and Koshland, 1972). Tactic responses of bacteria to temporal stimuli may be conceptually divided into a subsecond excitation process (Segall et al., 1982; Spudich and Koshland, 1975; Sundberg et al., 1986) followed by a slower adaptation process that gradually restores prestimulus behavior (Springer et al., 1979). The motile behavior of single bacteria has been quantitated by microscopy using three-dimensional tracking (Berg and Brown, 1972), photomicrography (e.g., Spudich and Koshland, 1975), and computerized video analysis (e.g., Sandberg et al., 1986). Single motor behavior has been studied by following the rotation of bacteria tethered onto glass coverslips. Responses of tethered bacteria to step, impulsive, exponential ramp, and sine-wave stimuli have been analyzed (Berg and Tedesco, 1975; Block et al., 1982, 1983; Segall et al., 1982, 1986). Iontophoretic application has been the only method published thus far that is sufficiently rapid for direct measurement of excitation times. Iontophoresis is restricted to the study of single, tethered bacteria and cannot conveniently be used for uncharged ligands such as serine.

Flash photolysis of caged compounds has emerged as a powerful technique for time-resolved analysis of intracellular signaling (Adams and Tsien, 1993). Here, we have applied this approach for the study of bacterial chemotactic excitation. Biologically inert 2-nitrobenzyl derivatives that photorelease serine and/or protons rapidly were synthesized, characterized, and used to study excitatory signaling. The flash geometries used provided uniform photorelease over whole fields of view. This allowed the flash photolytic approach to be coupled to the powerful, recently developed computer video analysis methods for cell tracking of entire bacterial populations. A large number of chemotactic mutants have been isolated or engineered since the last published measurements of excitation behavior (Segall et al., 1986). More than 50 mutant alleles are available in CheY alone (Bourret et al., 1990, 1993; Irikura et al., 1993; Oosawa et al., 1988; Roman et al., 1992; Sockett et al., 1992). These logistics make apparent the need for a fast, time-resolved behavioral assay to exploit fully the available mutant library for a mechanistic dissection of chemotactic signaling.

The drastic changes in the cell's swim-tumble balance that are effected as a rule by alteration of single protein components of the chemotactic machinery may mask effects of specific alterations upon signal processing. We have addressed this issue by examination of wild-type bacteria, wild-type bacteria with motor bias perturbed by physiological manipulation, and bacteria carrying mutations in chemotactic signal processing or motor proteins. Our data indicate that effects on signal processing times may be separated from effects on steady-state motility and response sensitivity. They provide additional support for current models of bacterial chemotaxis, but also reveal facets of excitation behavior that are not presently explained by such models.

MATERIALS AND METHODS

Preparation of caged 2-nitrobenzyl derivatives of protons and serine

2-Hydroxyphenyl 1-(2-nitrophenyl)ethyl phosphate, I

Caged H^+ was synthesized from *o*-phenylene phosphorochloridate and 1-(2-nitrophenyl) ethanol (prepared by borohydride reduction of 2-nitroacetophenone) followed by hydrolysis of the intermediate phosphate triester in the presence of 2,6-lutidine. The resulting mixture was separated on a 4- × 70-cm column of QAE-Sephadex A25 (for a synthesis using 12 mmol of each starting material) that was packed in the following manner. A 5 mM NaOH solution was mixed with an equal volume of methanol, and after brief degassing under partial vacuum (water pump) the Sephadex was added. The slurry was degassed again and packed into the column. The reaction mixture was applied to this column in 250 ml of the solution used to pack the column, and this was eluted with 1 liter of the same solution to remove uncharged substances. The column was developed by using a 4-liter (0.01–0.1 M) gradient of triethylammonium bicarbonate, pH 7.5. Caged H^+ was eluted as the second peak. After evaporation to dryness and repeated evaporation of methanol to remove triethylammonium bicarbonate, it was converted to its disodium salt by passage over Dowex 50 (Na^+-form) column in 40% overall yield. Caged H^+ was characterized by its ^1H NMR spectrum (recorded in D_2O-H_2O (9:1 v/v) with acetone as internal reference) at 500 MHz (on a Bruker AM500) at 25°C with a sweep width of 8 kHz in 16,000 data points. The ^1H NMR spectrum showed δ 6.13–7.72 (8H, Ar*H*), 5.70 (1H, m, ArC*H*), 1.53 (3H, d, CH_3). Caged H^+ had a titratable hydroxyphenyl group (pK 10.1) and the following ultraviolet (UV) absorption properties: at pH 7, ε 5.7 mM^{-1} cm^{-1} at λ_{max} 270 nm and ε 2.6 mM^{-1} cm^{-1} at λ_{min} 238 nm, and at pH 13, ε 10.3 and 6.0 mM^{-1} cm^{-1} at λ_{max} 236 nm and 285 nm, respectively, and 4.6 mM^{-1} cm^{-1} at λ_{min} 256 nm. High performance liquid chromatography on C_{18} reversed phase using an acetonitrile gradient in phosphate buffer (pH 6.0) showed caged H^+ to be homogeneous based on UV absorption at 254 nm.

2-Hydroxyphenyl phosphate, IV, the product of the photolysis reaction, was prepared by hydrolysis of methyl *o*-phenylene phosphate in water on an oil-bath maintained at 100°C for 1 h. Barium acetate was added to the solution which was then adjusted to pH 8 with NaOH. Some precipitation occurred, and the precipitate was removed and discarded. The product comprised a mixture of IV and presumed methyl phosphate in a molar ratio of 2:1 as determined by ^1H NMR. The second (i.e., weakly acidic) pK_a of the phosphate group in IV was determined by a combination of an acid-base titration of the mixture in water and by ^1H NMR spectroscopy in which the chemical shifts of the aromatic protons in IV were measured as a function of pH. IV also has pK_a of ~10 due to its phenolic group.

N-1-(2-Nitrobenzyl)ethoxycarbonyl-L-serine V

N-2-Nitrobenzyloxycarbonyl and related derivatives of amino acids were first described (Patchornik et al., 1970) as photolabile precursors for peptide synthesis, although these authors did not describe the serine derivative.

Caged L-serine was prepared and characterized as follows. A stirred solution of L-serine (285 mg, 2.7 mmol) in 0.25 M sodium hydroxide (11 ml) was cooled in an ice bath and treated simultaneously with a solution of 1-(2-nitrophenyl)ethyl chloroformate (1.25 g, 4.9 mmol) in dry tetrahydrofuran (24 ml) and 0.5 M potassium hydroxide (14 ml) for 10 min. The solution was stirred for a further 3 h at room temperature, then saturated with sodium chloride and extracted with diethyl ether. The aqueous phase was acidified to pH 2.5 with hydrochloric acid and extracted with ethyl acetate. The ethyl acetate extracts were washed twice with saturated sodium chloride solution, dried over Na_2SO_4, and evaporated to leave the crude product as a pale yellow oil. This was suspended in water (50 ml), neutralized with 1 M NaOH, and the solution was filtered. The yield was determined by quantitative UV spectroscopy at 263 nm (ϵ 4700 M^{-1} cm^{-1}) to be 1.28 mmol (47%).

For purification, the solution was lyophilized and the rçsidue redissolved in H_20 (8 ml). An aliquot (1 ml) was treated with sodium chloride (6 mg) and the solution was applied to a column of Sephadex LH-20 (2 × 40 cm) and eluted with water at 24 ml/h. Fractions (6 ml) were collected and analyzed by UV absorption and conductivity measurements. High conductivity was found in two peaks. The first (centered on fraction 22) contained little UV-absorbing material. The second centered on UV-absorbing fractions 25–28, which were combined, lyophilized, and redissolved in H_20 (1 ml). The concentration, determined by quantitative UV spectroscopy, was 106 mM. Contamination with free serine was 0.05%, as determined by amino acid analysis. The ^1H NMR spectrum (on a JEOL FX90Q) in D_2O showed δ 7.25–7.92 (4H, m, Ar*H*), 5.99 (1H, q, *J* 6.6Hz, ArC*H*), 3.84–4.00 (3H, m, CH_2CH), 1.50 and 1.52 (3H, 2× overlapping d, CH_3). The overlapping doublets for the methyl resonance correspond to the two diastereoisomers.

Preparation of motile bacteria

Vibrio alginolyticus was motility selected on soft agar and grown in liquid culture as described previously (Liu et al., 1990). They were harvested, washed three times, and resuspended in *Vibrio* motility buffer (0.1 mM 4-(2-hydroxyethyl)-1-piperazineethanesulfonic acid (HEPES), pH 7.5, 450 mM NaCl, 0.2% glucose). *Streptococcus* V4051 was grown in KTY medium, harvested, sheared and tethered in a flow cell, starved, valinomycin-treated, and energized as described previously (Khan et al., 1990). The 0.1 mM pH 7.5 phosphate buffer, of composition used previously (Khan et al., 1985) but containing 0.3 mM caged proton and 5 mM dithiothreitol in addition, was subsequently flowed in between 0.5 and 1 min after energization. *E. coli* and *S. typhimurium* strains were motility selected on soft tryptone agar, then grown in 10 ml Luria broth with antibiotic selection (25 μg/ml streptomycin for *E. coli*) in 100-ml flasks on a shaking water bath at 35°C. The strains were harvested at late-exponential phase, washed three times, and resuspended in weakly buffered motility medium (pH 7.0, 0.1 mM sodium phosphate, 67 mM NaCl, 10 mM KCl, 0.1 mM EDTA, 5 mM dithiotheitol, 5 mM sodium lactate, 125 μM L-methionine) for caged proton experiments and standard motility medium (pH 7.0, 10 mM sodium phosphate, 67 mM sodium chloride, 10 mM KCl, 0.1 mM EDTA, 5 mM dithiothreitol, 5 mM sodium lactate, 125 μM L-methionine) for caged serine experiments.

Flash spectroscopy

To effect photolysis of caged protons, up to 70 mJ of XeC1 (308 nm) Physik 201 Excimer laser light was focused onto the quartz sample cuvette with a set of fused silica cylindrical lenses. The energy of the 22-ns laser pulse was measured with the use of a GENTEC energy meter and a 7904 Tektronix oscilloscope. For the multiple-pulse experiments the excimer laser was run at about 1.6 Hz. The laser impinged on the 2-mm sample cuvette at an angle of 45° so that the pathlength was 2.83 mm. The measuring light from a tungsten-iodide lamp was passed through a Bausch and Lomb monochrometer so that it also impinged on the sample cuvette at 45° and 90° from the laser light. The effective aperture for the measuring light was 2 × 3 mm and laser light passed through the volume seen by the measuring light. The transmitted measuring light was detected by an EMI 9601B photomultiplier after passing through three type H dark blue glass filters (50% transmission at 421 nm) to reduce the scattered 308-nm laser light when observing the *aci*-nitro anion decay. When phenol red was monitored at 560 nm, four type 3661 B orange glass cut-off filters (each with 17% transmission at 560 nm) were used to reduce the scattered 308-nm laser light. The corresponding voltage signals from a 2.7 Kohm photomultiplier load resistor were amplified by a 7A22 Tektronix amplifier and displayed and photographed on a Tektronix 7904 oscilloscope or were digitized by a Nicolet 4094 oscilloscope and either photographed or plotted on an HP 7035B X-Y recorder. Increases in H^+ concentration were detected by the absorbance change at 560 nM of the H^+-indicator dye, phenol red (pK 7.6).

The photolysis kinetics of caged serine were measured in an absorption spectrophotometer linked to a frequency doubled ruby laser (347 nm) as described previously (Corrie et al., 1993; Walker et al., 1988).

Video microscopy of responses to flash photorelease

The bacteria were observed under dark-field (50 watt tungsten lamp). A 5× projection lens provided camera magnification such that a micrometer spanned about 1.5 video pixels. The Ultricon camera tube had low lag and high gamma (Inoue, 1986) suitable for tracking and contrast-enhancing rapidly moving bacteria. Five μl of sample with bacteria and caged compounds were contained in a bridged coverslip chamber. A custom-made 0.2-mm-thick quartz glass coverslip bridged two glass coverslips to form this chamber. For *E. coli* and *S. typhimurium* experiments, a density of about 20–40 motile bacteria per field of view was used. At higher densities tracking errors caused by, for example, crossover of paths of motile bacteria, became significant and, in addition, the motility of the bacteria on the microscope slide decreased precipitously after a few minutes due to oxygen depletion. In addition to a diffusion filter, a yellow filter (470 nm cut-off) was interposed between the lamp and sample to block blue light (Macnab and Koshland, 1974). Addition of up to 5 mM caged proton or caged serine from a pH-adjusted stock did not affect motility of the bacteria. The UV light used to effect photorelease was also filtered (see below), and the bacteria did not respond to the light in the absence of caged ligands. Absence of dithiothreitol elicited tumbling responses from *E. coli* and *S. typhimurium* upon flash photolysis which were probably due to formation of the 2-nitrosoacetophenone by-product III (Kaplan et al., 1978).

Amounts of caged compounds photoreleased on the microscope stage depended on the geometry for UV illumination. In one geometry, spatially uniform Kohler epiillumination of the sample by a continuous mercury arc lamp was controlled by an electronic shutter (Uniblitz, Vincent Associates, Rochester, NY). The light was filtered by a Nikon UV-2A (330–380 nm excitation, >400 nm barrier filters; 400 nm dichroic mirror) fluorescence cube and attenuated before passage through a 40× CF fluor objective lens of a Nikon Optiphot microscope. Alternatively, the discharge from a flash lamp was directed via a UV-transmitting fiber optic (Technical Video Ltd, Woods Hole, MA) onto the sample (Khan et al., 1992). An UG11 280–380 nm band-pass, with infrared reflective coating, filtered the light before entry into the fiber optic. The output end of the fiber optic was positioned at the focus of a 10-mm fused-silica lens (Ealing Optical), resulting in a spatially uniform, parallel output beam. An extra-long working distance 40× objective lens allowed illumination of the sample from an oblique angle of about 40°. A custom-made event marker put a 5-kHz tone recognizable by the EV Motion Analysis Software (MAS) (Motion Analysis Inc., Santa Rosa, CA) on the videotape and triggered the flash lamp, or the electronic shutter driver (Model D122, Vincent Associates). In biological experiments, a delay was interposed between the tone and the flash by means of a Grass stimulator to allow recording and analysis of prestimulus behavior.

The pH change due to caged proton photorelease was estimated using the pH indicator dye SNAFL1 (Molecular Probes Inc.). The SNAFL1 fluorescence intensity change was recorded onto videotape using a KS-1381 image intensifier, DAGE-MTI series 68 Ultricon camera, and Panasonic VHS-AG6300 recorder. The VP110 video digitizer threshold setting varied with the intensity of the recorded image and was used to read out the pH; after

calibration of the fluorescence with known pH buffers. The proton concentration was related to pH by acid-base titration of SNAFL1 and experimental buffers as described by Meister et al. (1987). In buffer containing 0.3 mM caged proton, approximately 33% (0.1 mM) was photolyzed by standard UV flash epiillumination (30-ms open shutter time, 50% transmittance ND filter) and approximately 10% (0.03 mM) by oblique, fiber optic guided lamp flash (200 watts) (Khan et al., 1992). In the former case an area not much greater than the field of view was illuminated and the pH change was rapidly offset (approximately 10 s) by diffusion of protons away to adjacent areas. All, or almost all, of the sample was illuminated by the UV flash in the latter geometry so that the pH or serine jump was stable for ~100 s.

Speed-up of tethered *Streptococcus* (Khan et al., 1990) and adaptation recovery times (Clarke and Koshland, 1979) provided independent bioassays for determination of the pH or serine jumps, respectively. *Streptococcus* V405197 was energized with a potassium diffusion potential equivalent to 1 pH unit (−58.8 mV). In this regime tethered cell speed is proportional to electrochemical potential (Khan et al., 1990). Speed-up upon flash photorelease was measured as described in Khan et al. (1985). The bacteria showed no measurable increase to the 0.03 mM proton jump produced by oblique flash illumination. Upon flash epiillumination, the fractional increase in speed was 0.49 ± 0.2 (n = 10), indicating a pH change of this magnitude. This value is higher than that estimated by SNAFL1 measurements (approximately 0.35 units), but is likely to be a overestimate due to the fact that proton photorelease was about a minute after energization at which time the electrochemical potential in the artificially energized cells is approximately 20% less than the imposed diffusion potential (Khan et al., 1985). Recovery times were measured for large serine jumps using oblique flash illumination. The estimated serine release was approximately twofold greater than the proton release measurements using SNAFL1, in agreement with the difference in quantum yields of the two caged compounds. Thus, wild-type *E. coli* had, for example, a recovery time of 24 ± 3 s upon oblique flash photolysis of 40 μM caged serine indicating photorelease of ~8 μM serine (Clarke and Koshland, 1979). Serine in the caged serine sample was estimated by recovery time measurements to be <1%.

Computer-assisted motion analysis

Bright objects were thresholded out by the VP110 digitizer and this information used by the MAS software to calculate centroids for each discrete object within a frame and subsequently to link centroids from frame-to-frame into paths as detailed in Sundberg et al. (1986). Both linear (SPD) and angular (RCD) speeds have been used to study *E. coli* motile behavior (e.g., Tisa et al., 1993). SPD, expressed in $\mu m \cdot s^{-1}$, is the absolute linear speed of a path obtained by multiplying the frame-to-frame displacement by the number of frames digitized per second. RCD, expressed in $^\circ \cdot s^{-1}$, is the absolute angular rate of change of direction of a path from frame-to-frame multiplied by the number of frames digitized per second. The discrimination by these parameters of motile and immotile objects varied with the digitization rate (Fig. 1 *a*). Latex beads (1.065 μm diameter; Polysciences Inc.) were used to evaluate the video instrumentation. Stuck beads had a frame rate-independent SPD (<1 μm/s) and high RCD due to sync imprecisions between successive video frames (Inoue, 1986). Frequency filtration abolished this error, but also decreased temporal resolution and was, therefore, avoided. Beads free in solution had a frame rate-dependent SPD. The slope of x^2 versus time, t, where x = SPD/t, was 1.711 × 10^{-9} cm^2/s. The proportionality constant obtained by dividing the slope by the diffusion coefficient (4.06 × 10^{-10} cm^2/s) was 3.9. Immotile objects the size of bacteria are perceived by the optoelectronics as undergoing two-dimensional diffusional drift. The image depth of field was determined empirically. First, the angular travel of the focus knob corresponding to the depth of the bridged coverslip chamber (0.17 ± 0.02 mm) was determined by focusing alternately on bacteria stuck on the slide and top coverslip undersurface. Second, the knob travel needed to defocus stuck bacteria to prevent digitization was then used to estimate an effective depth of field of about 10–15 μm, or 10 times the mean body length of the bacteria. Thus, the digitized video images provided two-dimensional projections of the three-dimensional trajectories of motile bacteria.

Immotile objects were filtered out using a dummy file (Sager et al., 1988). For *V. alginolyticus* (SPD = 36.4 ± 7.8 μm/s), the video records were digitized at 60 frames/s and motile bacteria were separated from immotile objects using a SPD threshold of 25 μm/s. Individual reversals could be

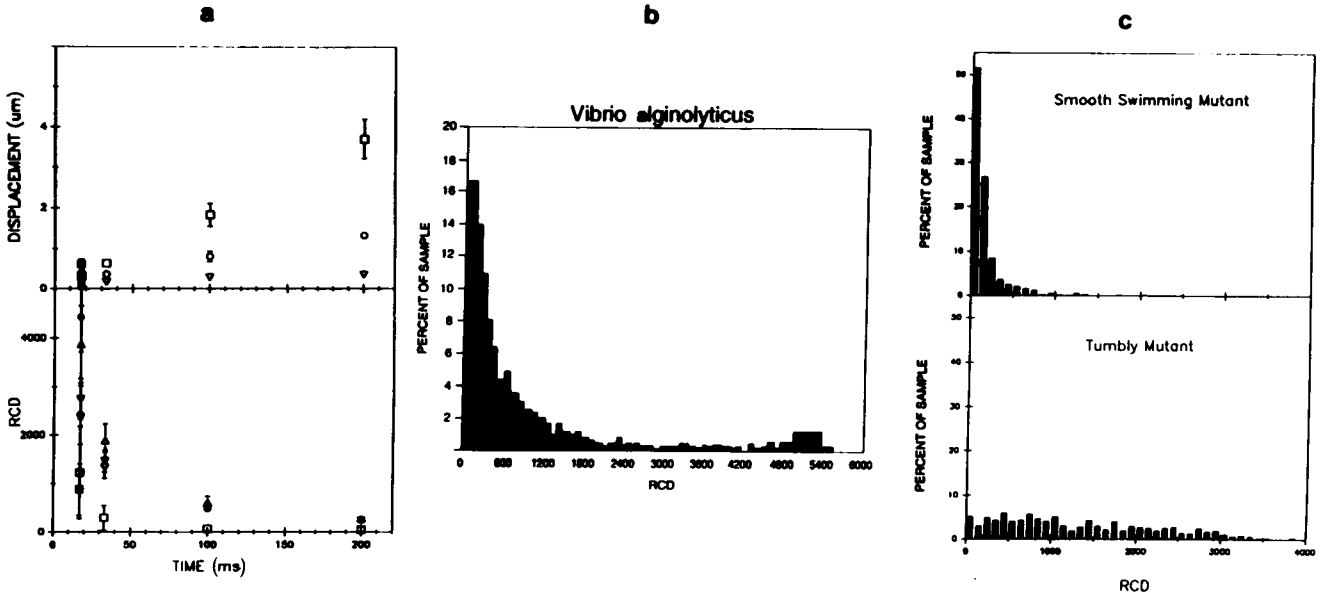

FIGURE 1 Computer measures of motile behavior. (*a*) Video images of stuck beads (*triangles*), beads free in solution (*inverted triangles*), tumbly mutant *S. typhimurium* SL4041 (*circles*), and smooth swimming *E. coli* HCB437 bacteria (*squares*) were digitized at four different sampling frequencies: 5, 10, 30, and 60 frames/s. *V. alginolyticus* video images (runs, *closed squares*; reversals, *closed circles*) were digitized at 60 frames/s. (*Top*) The displacement, x, is plotted against the time between successive digitized frames, t. (*Bottom*) The RCD is plotted against t. (*b*) Histogram of frame-by-frame RCD values of a *V. alginolyticus* population of more than 1000 paths. (*c*) Histograms of frame-by-frame RCD values of *E. coli* and *S. typhimurium* mutant populations of more than 1000 paths. (*Left*) Smooth swimming *E. coli* HCB437. (*Right*) Tumbly mutant *S. typhimurium* SL4041.

identified using an RCD/SPD ratio (Sundberg et al., 1986). A randomly selected population (n = 20) of reversal events had a mean RCD and SPD of 4414 ± 693°/s and 5.34 ± 4.1 μm/s, respectively (Fig. 1 *a*). Reversal events gave rise to a distinct peak around 80°/frame in the RCD population histogram (Fig. 1 *b*). Therefore, within any given frame-to-frame interval, a path was identified as undergoing a reversal if its RCD and SPD were greater than 60°/frame and less than 10 μm/s, respectively. For measurement of the excitation response, the frame-to-frame ensemble mean reversal frequency was computed, analogous to the computation of ensemble mean rotation bias (Block et al., 1982). The resulting files were smoothed after the computation by three-frame averaging. Smoothing of individual paths (Marwan and Oesterhelt, 1990; Sundberg et al., 1986) was omitted because this affected measurement of the rapid response kinetics of the bacterial species studied here.

Comparison of *E. coli* and *S. typhimurium* mutants (Fig. 1) showed that SPD is a good discriminator of smooth-swimming and tumbly behavior at low, but not high digitization frame rates in which the RCD is more effective. Time-resolved measurement of excitation required high digitization rates (>30 frames/s). Therefore, the RCD/SPD ratio was used to filter out immotile objects, whereas the RCD was used as a measure of *E. coli* and *S. typhimurium* motile behavior. RCD population histograms of smooth-swimming and incessantly tumbly bacteria (Fig. 1 *c*) overlap but are clearly distinguishable.

The RCD provided an intuitively satisfactory measure of tumbling. Video digitization of smooth-swimming mutant bacteria (e.g., HCB437, ST112), slowed to various extents by addition of uncoupler (CCCP, Sigma Chemicals Co., St Louis, MO), showed that cell trajectories were better resolved at higher speeds, with an RCD-SPD correlation of $-37.06° \cdot \mu m^{-1}$. We standardized for vigorous motility of experimental cultures by harvesting them at the same growth phase and documenting their population SPD. To establish the RCD as a quantitative measure of cell motile behavior, we related it to motor rotation bias (Table 1, Fig. 2). Three regimes were distinguished. From 1 to 0.35 CCW rotation bias, the RCD varied approximately linearly with motor bias. The regime from 0 to 0.35 CCW bias corresponded to the tumbly swimming phenotype over which the RCD plateaued as a function of motor bias. A third regime of inverse swimming motility (Khan et al., 1978) has been studied little. Effects of inverse motility on population RCD and SPD could be documented (Table 1), but not expressed in terms of tethered cell rotation bias which had saturated. Thus, swimming in such mutant populations was enhanced upon decreasing intracellular pH, a manipulation known to enhance CW rotation (Kihara and Macnab, 1981; Repaske and Adler, 1981). For small amplitude inverse-normal motility transitions, SPD proved a more sensitive measure of excitation behavior than change of RCD. Small differences in tethered cell rotation bias of these mutant strains were documented when a greater number of tethered cells was studied (Khan et al., 1978). It is possible, however, that the cultures used here had a greater proton-motive force, and hence CW/CCW bias (Khan and Macnab, 1980), due to the presence of lactate in the medium.

RESULTS

Mechanism and kinetics of caged proton photolysis

Fig. 3 illustrates H^+ release on photolysis of caged H^+ at pH 6.8. The proposed mechanism (Fig. 3 *a*) describes intermediate II which is chromophoric and is presumed to be an *aci*-nitro anion possibly in rapid equilibrium with other species by analogy with the corresponding intermediate formed during caged ATP photolysis (Walker et al., 1988). Increases in H^+ concentration were detected by the absorbance change at 560 nm of the H^+-indicator dye, phenol red (pK 7.6). The $[H^+]$ change that occurs is a step release of protons in <5 μs. Previous work (Walker et al., 1988) with a frequency-doubled ruby laser and caged ATP also indicated that the proton step concentration jump occurs in <5 μs. It follows that $k_1 > 10^5\ s^{-1}$ (Fig. 3 *a*). Fig. 3 *b* record *A* illustrates H^+ release after a 60-mJ excimer laser pulse at 308 nm to photolyze caged H^+. Control experiments recorded at 560 nm are shown in record *B* (no phenol red) and record *C* (no caged H^+). The absence of a spectral change in record *B* indicates that II has zero absorbance at 560 nm like caged H^+. The small effect when caged H^+ is omitted (record *C*) is probably due to photobleaching of phenol red.

From the spectral change in Fig. 3 *b* that corresponded to 26 μM increase in the imidazolium ion concentration and a

TABLE 1 Computer measures of motile behavior and motor rotation bias of *E. coli* and *S. typhimurium* strains RCD and SPD standard errors were ~100°·s⁻¹ and 2 μm·s⁻¹ respectively. Single cultures were used for each measurement relating tethered cell CCW rotation bias (the mean CCW interval divided by the sum of the mean CW and CCW intervals) to swimming cell RCD and SPD. Between 10 and 20 tethered cells and more than 200 swimming cell paths were used for each measurement.

Strain	Relevant genotype	Bias	RCD (°·s⁻¹)	SPD (μm·s⁻¹)
HCB437[a]	Δ(tsr)7021 Δ(trg)100 zbd::Tn5 Δ(cheA-cheZ)2209	1	426	19.3
RP8611[b]	Δ(tsr)7028 Δ(tar-tap)5201 Δ(trg)100 zbd::Tn5	1	445	17.5
RP3851[b]	Δ(tar)386-2 tsr::Tn5	0.93	556	16.0
RP2361[b]	Δ(tar)386-2	0.86	613	16.2
RP2859[b]	Δ(tap-cheB)2241	0.85	669	16.7
RP437[b]	Wild-type	0.77	648	17.0
RP437*	—	0.70	681	18.8
RP437‡	—	0.52	906	17.1
AW677[c]	cheB287	0.355	977	16.0
RP1616[b]	Δ(cheZ)6725	0.08	910	15.9
SL4041[d]	cheB411	0.01	1091	16.2
ST120[d]	fliG (181RD)	0	1108	15.8
ST134[d]	fliM (185GD)	0	942	13.8
ST120‡	—	0	670	11.3
ST134‡	—	0	620	11.5

Strain references: Parental strains *E. coli* RP437 (Parkinson, 1978) and *S. typhimorium* LT2 (Vary and Stocker, 1973) were wild-type for motility and chemotaxis. *a*, Wolfe et al. (1987); *b*, J. S. Parkinson (personal communication); *c*, Repaske and Adlers; *d*, Irikura et al. (1993) and Khan et al. (1978).
* Grown for 2 h at 22°C before harvest.
‡ Buffer = standard motility medium at pH 6.0 containing 30–50 mM acetate.

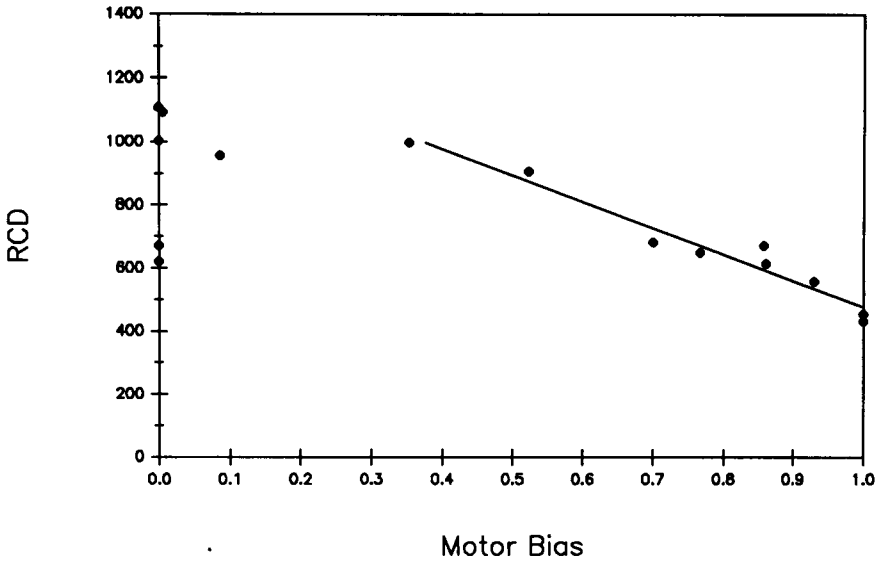

FIGURE 2 Correlation between swimming cell RCD and tethered cell rotation bias. Plot of the relation between tethered cell CCW rotation bias and swimming cell RCD values. The best-fit line to the data between 0 and 0.645 CCW bias is shown. Table 1 lists the strains used. *E. coli* HCB437 and *S. typhimurium* SL4041 represented the two extremes of smooth-swimming and tumbly behavior. Their mean population RCD values, as estimated from further measurement of more than 1000 motile paths taken from three different cultures in each case, were 350 ± 50°/s and 1150 ± 50°/s, respectively.

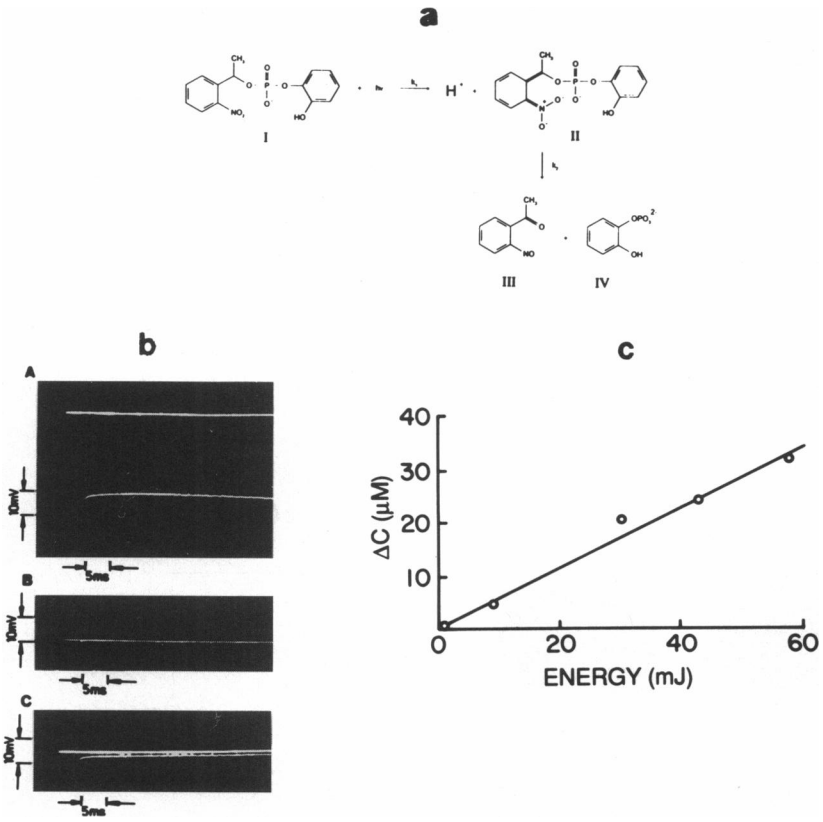

FIGURE 3 Excimer laser photolysis of caged H^+. (*a*) Mechanism of photolysis of caged proton. (*b*) Photolysis kinetics. pH changes were measured by the H^+ indicator dye, phenol red. Reactions were monitored at 560 nm in solutions consisting of 50 mM KCl, 4 mM EGTA, 1 mM imidazole-HCl at 22°C and pH 6.8 and in addition in (*A*) 0.4 mM phenol red plus 0.4 mM caged H^+; in (*B*) 0.4 mM caged H^+; in (*C*) 0.4 mM phenol red. The initial transmission corresponded to 250 mV and is shown as the upper trace in each case extending the full width of the experimental record. In the experimental trials the initial absorbance during the first 5 ms was as in the upper traces. The laser pulses occurred at 5 ms and were accompanied by a 0.06 and a 0.003 decrease in absorption (from 0.46) in records *A* and *C*, respectively (pathlength 2.83 mm). In record *B* the initial absorbance was zero and no change occurred on the laser pulse. (*c*) Photolysis yield. Concentration increase (ΔC) in μM of the protonated species of phenol red measured at 560 nm as a function of laser energy (in mJ) impinging on the sample. In this case 80% of the energy was absorbed by the sample. Sample conditions: 0.4 mM caged H^+ plus 0.4 mM phenol red, 21°C and pH 7.6.

5 μM increase in that of the protonated form of phenol red, the pH jump change from 6.8 was 0.05. In this experiment there were two buffers present: 1 mM imidazole (pK 6.95), 0.4 mM phenol red (pK 7.6), as well as the photolysis product IV (pK 5.3).

The experiment was repeated without imidazole at pH 7.6 (Fig. 3 *c*). At 60-mJ laser energy the decrease in pH was 0.14 corresponding to a 32 μM increase with protonated form of phenol red. Fig. 3 *c* also shows the dependence of number of photolytically produced protons as a function of energy of the incident laser pulse. From the slope of this curve, $Q_{308\ nm}$, the effective quantum efficiency for the production of protons from the excimer laser pulse can be determined as the number of protons produced divided by the number of pho-

tons absorbed. Thus

$$Q_{308\,nm} = N_o Vhc\alpha/\lambda GF(1 - T)$$

where N_o is Avogadro's constant, V is the sample volume in liters, h is Planck's constant, c is the velocity of light, λ = 308 nm, the wavelength of the incident photons, G is a geometrical factor for the cell arrangement (equaling 1/2 in this case), T is the transmission through the sample cell, and α is the slope of the line in Fig. 3 *c*. The factor $F = \epsilon_1/(\epsilon_1 + \epsilon_2)$, where ϵ_1 is the extinction coefficient of caged H^+, and ϵ_2 is the extinction coefficient of phenol red at pH 7.6 each at 308 nm. The data in Fig. 3 *c* were fitted to a least squares line from which α = 0.564 μM/mJ and from the experimentally measured transmission of the sample (0.2) and the equation given above the $Q_{308\,nm}$ was calculated to be 0.095. This is to be compared with a value for quantum efficiency obtained by measuring the ratio of the absorbance amplitudes at 435 nm of the *aci*-nitro anions formed during photolysis of caged H^+ and caged ATP by 300–350 nm light from a Chadwick Helmuth Strobex model 238 Xenon arc flashlamp. The ratio was then multiplied by the quantum efficiency for caged ATP (0.63) (Walker et al., 1988), that in turn was obtained from the actinometric measurement of quantum efficiency of 1-(2-nitrophenyl)ethyl phosphate (0.54) (Kaplan et al., 1978). By this method the quantum efficiency for photolysis of caged H^+ is 0.29 ± 0.02. An assumption in this latter method is that II has the same extinction coefficient as the *aci*-nitro anion produced in the photolysis of caged ATP. It has been suggested that the lower quantum efficiency at 308 nm may be associated with a greater Π-Π* contribution to the absorption band (McCray and Trentham, 1989).

Fig. 4 *a* demonstrates that the rate constant k_2 (Fig. 3 *a*) of decay of II in the photolysis of caged H^+ has a pH dependence similar to that of caged ATP (Walker et al., 1988), in which the decay rate is proportional to $[H^+]$ below pH 8. The section from pH 7.5 to 5.5 of the pH profile was fitted to a least squares line: $\log\{k_2/(s^{-1})\} = 8.634 - 0.988$ pH. To be able to produce a significant pH jump the concentration of buffer was decreased to 0.1 mM. Fig. 4 *b* shows the result of a multiple excimer laser pulse experiment in which the laser was run in the repetitive mode with one laser pulse every 6 s. The records *A–D* show the first to fourth laser pulse on the same sample and illustrate that the decay rate of the *aci*-nitro intermediate increases and that the amplitude of the transmission change due to II decreases with each pulse (Fig. 4 *c*). The rates obtained from Fig. 4 *b* were used with the pH profile curve in Fig. 4 *a* to determine the new pH values after each laser pulse which are also recorded in Fig. 4 *c*. The pH first decreases by approximately 1 pH unit at a time through the range of 8 to 6 and then tends to a plateau at about pH 5 as expected from the pK (5.3) of the product 2-hydroxyphenyl phosphate IV. The pK (5.3) of the photolysis product 2-hydroxyphenyl phosphate precludes caged H^+ being used to make solutions more acid than about pH 5. The charged state of caged H^+ and hence its presumed membrane impermeability means that it may be used to release protons in defined cellular compartments thereby setting up proton gradients across membranes. Thus, the compound has been used to study energization of flagellar rotation in a motile *Streptococcus* (Khan et al., 1985; Shimada and Berg, 1987). Another caged proton (Janka and Reichert, 1987) and a caged hydroxide (Irie, 1983) have been described, but these compounds are perhaps more likely to partition into biological membranes and/or

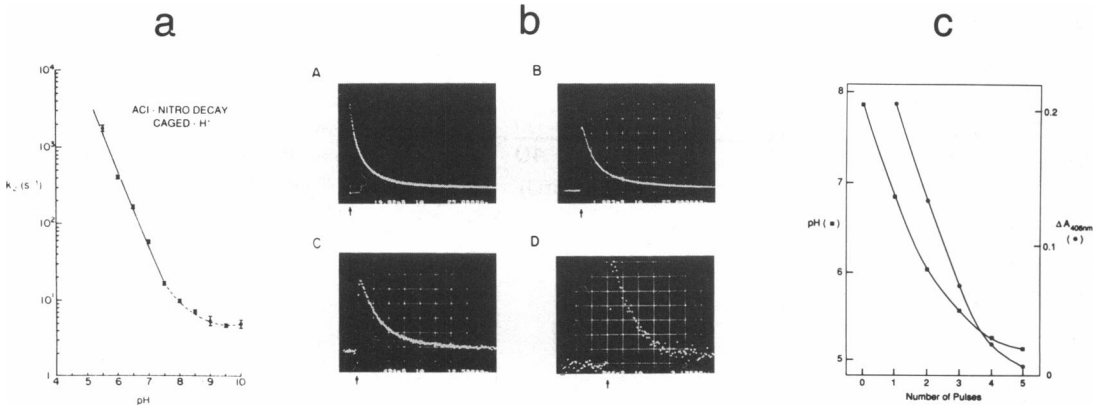

FIGURE 4 Photolysis of caged H^+ as a function of pH. (*a*) First order decay rate constant (k_2, Fig. 3 *a*) (s^{-1}) of the *aci*-nitro anion intermediate II, plotted on a log scale as a function of pH. Solution conditions: 1 mM caged H^+ (Na^+ salt) in buffers (histidine, imidazole, Tris, or borate as appropriate) at ionic strength 0.45 M and 22°C. (*b*) Absorption changes of II at 406 nm after the first four excimer laser pulses in a multiple excimer laser pulse experiment showing the increased decay rates of the *aci*-nitro intermediate as the pH falls. Vertical and horizontal scales are respectively: (*A*) 25 mV (ΔA = 0.028) per division and 19.82 ms per division; (*B*) 25 mV per division and 1.983 ms per division; (*C*) 12.5 mV (ΔA = 0.014) per division and 494 μs per division; (*D*) 3.1 mV (ΔA = 0.0035) per division and 246 μs per division. The initial transmission corresponded to 400 mV. Times of the laser pulses are indicated by arrows. Sample conditions: 1 mM caged H^+, 0.1 mM Tris buffer, 22°C with pH initially at 7.9. (*c*) pH (*squares*) occurring immediately after each laser pulse and the corresponding relative maximum absorption (*circles*) of the *aci*-nitro anion formed on each pulse. *b* and *c* record data taken from the same experiment.

be membrane permeable. In addition, the pH-dependent rate of the decay of II can be used as an intrinsic pH meter to measure the pH jump produced.

Mechanism and kinetics of caged serine photolysis

The structure of caged L-serine is shown in Fig. 5 *a* together with the probable mechanism of its photolytic decay to L-serine and by-products, III and CO_2. Evidence for the mechanism is described in the legend to Fig. 5 based on the spectral signals inferred as being due to the formation and decay of VI (Fig. 5 *b*) and on the proton stoichiometry (Fig. 5 c_1 and c_2). The product quantum yield of caged serine, measured by comparison with the P^3-1-(2-nitrophenyl)ethyl ester of ATP (caged ATP) (Walker et al., 1988) was 0.65 (±0.05). The kinetics over the pH range 4 to 8 have been studied in detail for the corresponding caged L-glutamate (Corrie et al., 1993), and identical results were obtained with caged L-serine. In the pH range 5.5 to 8 the rate constant of L-serine release is proportional to $[H^+]$ being 17 s^{-1} at pH 7.0 under the conditions of Fig. 5. More rapid release of serine was therefore achieved in the biological experiments conducted at pH 6.0.

Computer measurement of *V. alginolyticus* excitation response

This bacterium was used to test whether whole fields of view of rapid-swimming bacteria could be tracked at high temporal resolution by computer. A system that tracks rapidly swimming bacteria one cell at a time has been described (Poole et al., 1988). *V. alginolyticus* motile behavior is directly related to the rotation of its single flagellum which alternately pushes or pulls the cell. *V. alginolyticus* reversed about once per second. Upon proton photorelease, its reversal frequency increased to about 3 per second (Fig. 6 *a*). The rapid response ($t_{½}$ = approximately 50 ms) was due to the pH change. No response was observed in strongly buffered

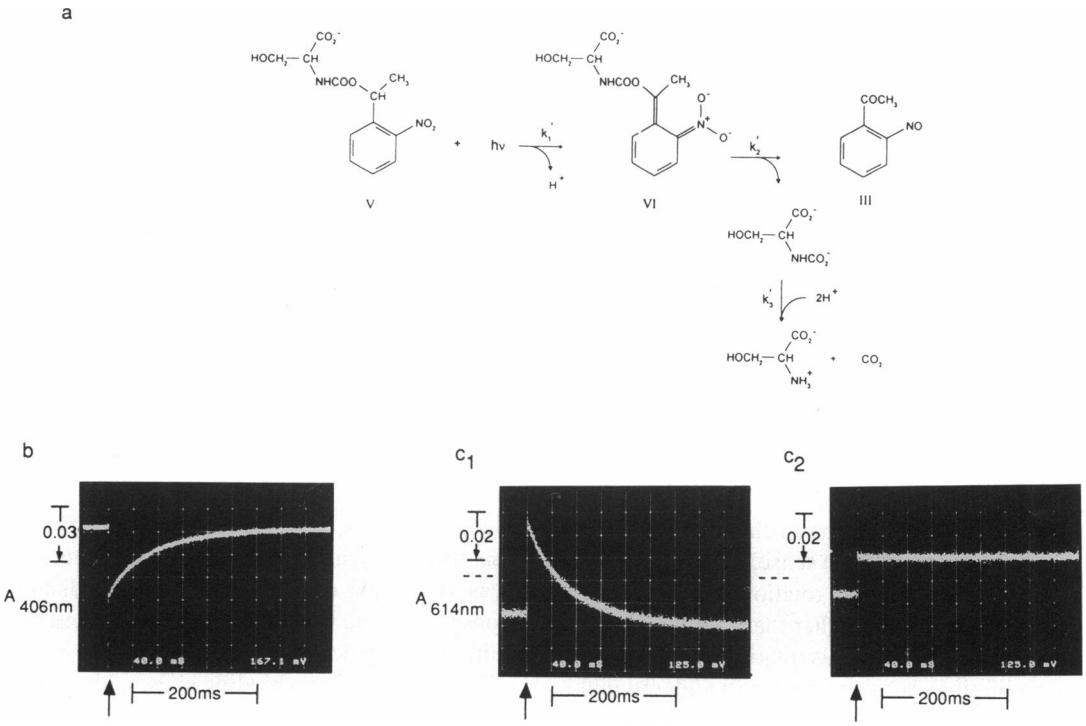

FIGURE 5 Photolysis of caged serine V. (*a*) Minimal mechanism of caged serine photolysis. Formation (step 1) and decay (step 2) of intermediate VI, an *aci*-nitro anion, were monitored from its absorption band (peak at 406 nm). Proton release (step 1) and uptake (step 3) were monitored using the pH indicator bromothymol blue at 614 nm, the absorption maximum of the basic form, at which wavelength neither the acidic form of bromothymol blue nor VI absorb. (*b*) Spectrophotometric record at 406 nm showing formation and decay of VI. The aqueous solution at 21°C contained 0.1 mM caged L-serine, 100 mM KCl, 1 mM dithiothreitol, and 1 mM 1,4-piperazine-*N*,*N*′-bis(ethanesulfonic acid) at pH 7.0. (c_1) Spectrophotometric record at 614 nm showing release and uptake of protons. The aqueous solution at 21°C contained 0.2 mM caged L-serine, 100 mM KCl, 1 mM dithiothreitol, 1 mM 1,4-piperazine-*N*,*N*′-bis(ethanesulfonic acid) at pH 7.0 and bromothymol blue (absorption 0.75, 4-mm-pathlength cell). (c_2) Control spectrophotmetric record at 614 nm showing photobleaching of bromothymol blue due to laser flash. The solution was as in record c_1 except that no caged serine was present. The arrows mark the time of the laser pulse. The dashed lines in record c_1 show the photobleaching correction to be applied to the initial absorption of bromothymol blue (obtained from record c_2). After the correction is applied the initial release of a proton followed by two-proton uptake is apparent (CO_2 hydration and HCO_3^- formation occur much more slowly (Ho and Sturtevant, 1962; Wang et al., 1972)). The rapid initial increase and decrease in absorption in *b* and c_1, respectively, indicate $k'_1 > 10^5$ s^{-1} (limited by the time resolution of the flash spectrometer). Because the rate constants of the slower phases in *b* and c_1 are approximately the same, $k'_3 > k'_2$ and $k'_2 = 17$ s^{-1}. The kinetics of serine release from caged serine were measured from pH 4.0 to 8.0 and were indistinguishable from those of glutamate from the corresponding caged glutamate (Corrie et al., 1993).

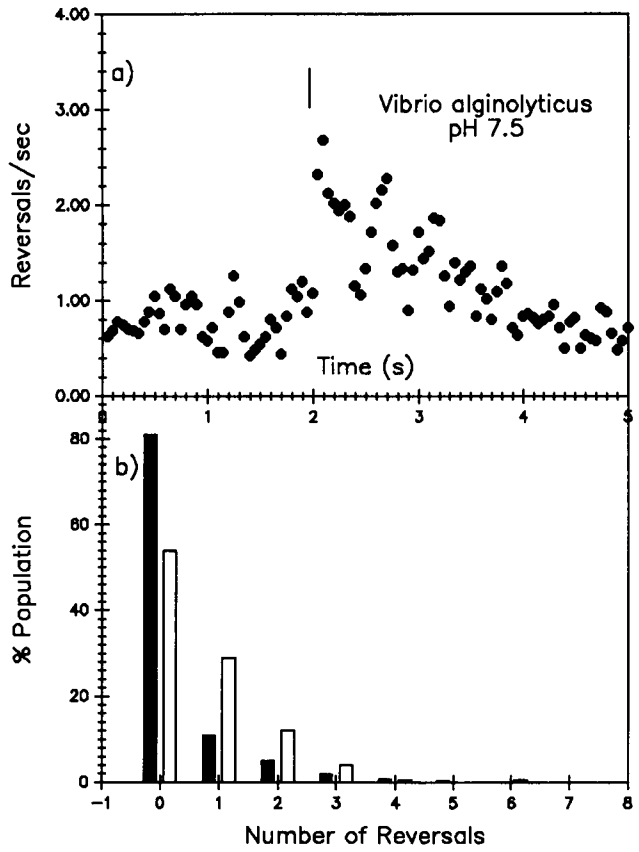

FIGURE 6 *V. alginolyticus* excitation response. (*a*) The excitation response of more than 1500 motile paths to photorelease of 0.1 mM caged protons resulting in a pH change of about 0.35 units is shown. Vertical bar marks flash. (*b*) Post- and prestimulus histograms of the half-second poststimulus (*open bars*) and prestimulus (*closed bars*) periods of the number of reversals per path for the data shown.

(50 mM HEPES) media. A pH change of 0.35 units produced a maximum peak response. Greater pH changes increased response duration but not amplitude. Only half of the population responded (Fig. 6 *b*), but part of the population showed multiple reversals. One interpretation of this observation is that acid pH jumps favor one rotation sense, akin to the effect of chemoeffectors on *E. coli* motor rotation bias, but effect destabilization of the unfavored, rather than stabilization of the favored state. Because prestimulus rotation intervals have a subsecond mean lifetime, some bacteria will undergo multiple reversals poststimulus. The rapid, sensitive response of this bacterium to pH is of interest because its motility is powered by sodium ions. Thus, pH sensing in this species must be independent of the energization of the flagellar motor, a possibility raised in the literature (see Macnab, 1987). Furthermore, the data show that *V. alginolyticus* exhibits rapid processing of pH change signals.

Excitation responses of *E. coli* to Tsr repellent and attractant stimuli

We studied two features of the chemotactic response to step stimuli: response amplitude and response time. The response amplitude was defined as the maximum change in the population RCD elicited by the stimulus. The response time was defined as the time required to achieve the half-maximal change of RCD. It is equivalent to the reaction half-time ($t_{1/2}$) parameter used in chemical reaction kinetics. The step jumps effected by ligand photorelease were controlled and measured with ease, allowing study of subsaturation responses. Saturation responses were recorded when the population RCD transiently attained a value equal to that of smooth-swimming and incessantly tumbly mutant populations for attractant (serine) and repellent (pH) stimuli, respectively. Larger pH jumps proved unsuccessful in driving the repellent response into the inverse-swimming regime. RCD values obtained during the response measurements, in fact, exceeded the mutant population RCD measurements at either extreme by about 100°/s. In addition to intracellular signaling chemistry, motile behavior depends on mechanical factors, such as cell size and number of flagella per cell, which may account for the differences observed.

Fig. 7 shows *E. coli* responses to caged proton photorelease. A Tar deletion strain was used because Tar mediates smooth-swim responses to protons (Bourret et al., 1991). Subsaturation responses with reduced amplitude and increased response time were elicited by small pH jumps. The subsaturation data established that the chemical perturbations that determine motor response are complete within 1 s. Inasmuch as perturbation of internal pH to rapid pH change requires many seconds for completion (Slonczewski et al., 1982), these data implied that tumbling is initiated by extracellular binding of protons to Tsr.

Fig. 8 extends our initial documentation of *E. coli* responses to caged serine photorelease (Khan et al., 1992). The response is specific for serine because a mutant lacking Tsr does not respond (Fig. 8 *b*). As for repellent stimuli, a modest increase in response time accompanied reduction in response amplitude (approximately twofold increase for a roughly corresponding decrease in amplitude upon 0.4 μM serine photorelease). Once maximal response amplitude was achieved, larger serine jumps did not affect response kinetics, but only response duration, i.e., recovery times. Saturation responses, measured at pH 6.0 and pH 7.0, had indistinguishable response times and were, therefore, not limited by caged serine photolysis kinetics.

Tsr has at least two binding sites, with different affinities, for serine; occupancy at both sites has behavioral effects as documented by increases in response duration (Clarke and Koshland, 1979). However, response amplitude saturated in the micromolar range corresponding to half-occupancy of the high-affinity site. Thus the response sensitivity of wild-type bacteria toward serine was comparable with that reported for aspartate (Weiss and Koshland, 1988). We estimated the fractional change in Tsr receptor occupancy from subsaturation response amplitudes given Tsr-serine binding affinity (Clarke and Koshland, 1979), the amount photoreleased, and the <1% serine contamination of the caged serine. The change in RCD was related to the percent change in motor bias (Fig. 2). The gain, defined as the ratio of the change in

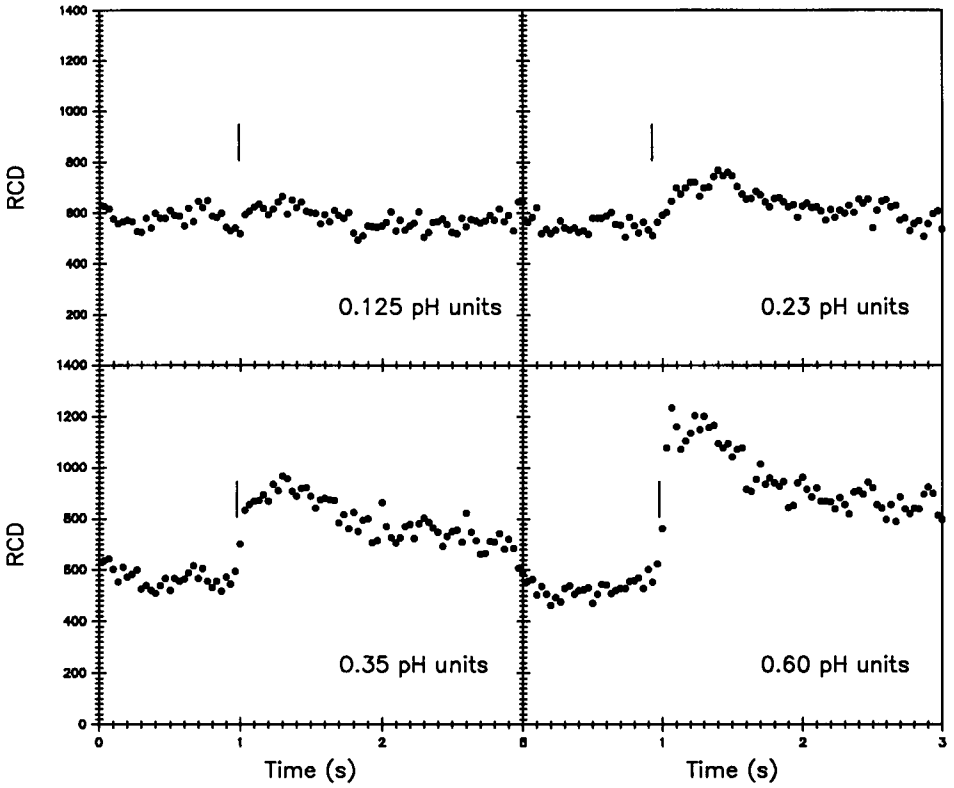

FIGURE 7 Excitation responses of *E. coli* to photorelease of caged proton. Strain RP2361 (Tar$^-$) was used. Estimated pH jumps are denoted on the bottom right of each panel. Each panel represents more than 1000 motile paths. Vertical bars mark flashes. Data segments between flash and intervals at which maximal, or minimal, RCD values were reached were identified by eye and fitted by polynomial functions for estimation of response times. Maximal responses, obtained upon jumps of 0.35 or > pH units, reached RCD values corresponding to incessantly tumbly mutant populations (Fig. 2) and response times of ~0.05 s. For a pH jump of ~0.23 units, the response time increased (0.11 ± 0.01 s) and amplitude decreased approximately two- to threefold.

motor bias over the change in receptor occupancy following Segall et al. (1986), was approximately 6. This estimate is an order of magnitude lower than that reported for responses of the analogous chemoreceptor, Tar, toward aspartate (Segall et al., 1986). The matter merits further study.

Excitation behavior dependence on motor rotation bias

A number of chemotactic mutants with abnormal swim-tumble balance have high response thresholds (Block et al., 1982). However, CheR-CheB double deletion mutants, with normal swim-tumble balance but high response thresholds have also been described (Segall et al., 1986). We investigated the excitation behavior of CheR-CheB mutant strains to both attractant (serine) and repellent (protons) stimuli. We further studied excitation behavior when motor bias was altered by perturbation of metabolic parameters, by mutation of the Che proteins, and of the motor proteins implicated in switching of rotation sense. The occurrence of different affinity Tsr serine binding sites proved to be advantageous because responses could be studied over a wide range of stimulus strength, allowing separation of effects of response sensitivity from response kinetics.

CheR-CheB mutant strains have been the subject of lively controversy in the literature as regards differences in excitation behavior from wild-type bacteria (Segall et al., 1986; Stock and Stock, 1987). Fig. 9 shows responses of a CheR-CheB strain to serine. The reduced sensitivity (approximately 50-fold) was comparable with that reported for responses of CheR-CheB strains to aspartate (Segall et al., 1986), but saturation response times were indistinguishable from those of wild-type bacteria. The strain also had reduced sensitivity for repellent stimuli. No response was observed for pH jumps known to produce saturation responses in wild-type bacteria. Receptor control of CheA kinase activity is modulated by methylation state and ligand binding (Borkovich and Simon, 1992). We sought to determine whether the reduced response sensitivity of CheR-CheB deletion strains could be mimicked in wild-type bacteria adapted to saturating concentrations of other Tsr ligands. No differences in responses to 0.2 pH unit jumps in the presence and absence of 10 mM leucine (Tsr repellent) or 5 mM α-aminoisobutyrate (Tsr attractant) were observed. Likewise, no difference in response to photorelease of 5 μM serine in the presence or absence of 10 mM leucine was observed. These data imply that the effects of receptor methylation and ligand binding on CheA activity cancel completely leaving signal generation due to binding of other ligands unaffected. Alternatively, it is possible that modulation of CheA activity does not determine response sensitivity.

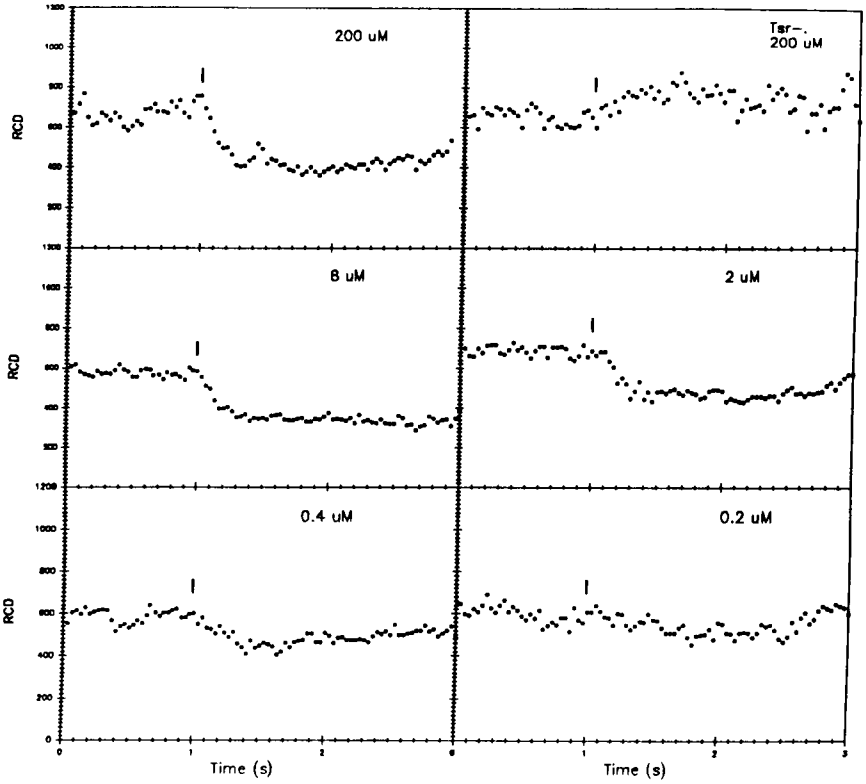

FIGURE 8 Excitation responses of *E. coli* to photorelease of caged serine. Wild-type strain RP437 was used except for data in the top right panel that show RP5700 Δ(tsr)7021 (Ames and Parkinson, 1988) response to serine photorelease. Serine concentrations photoreleased are denoted on the top right of each panel. Each panel represents more than 1000 motile paths. Vertical bars mark flashes. Maximal response amplitudes reached RCD values corresponding to completely smooth-swimming mutant populations (Fig. 2) with ~0.12-s response time (determined as in Fig. 7). The response to 0.4 μM serine photorelease had half-maximal amplitude and increased response time (0.23 ± 0.03 s). For each experimental culture, the baseline RCD corresponding to smooth swimming of the entire population was determined by recording smooth-swimming responses of the bacteria upon rapid mixing with 1 mM serine. Baseline RCD values were ~400°·s⁻, in agreement with values obtained for smooth-swimming mutants.

Wild-type *E. coli* were made tumbly (RCD ~900°·s^{-1} (Table 1) by acidification of internal pH, while still maintaining vigorous motility (Kihara and Macnab, 1981). These bacteria had reduced response sensitivity requiring photorelease of >20 μM serine for a strong response (RCD <600 °·s^{-1}), but response times were unaffected. Tumbly CheB (*S. typhimurium* SL 4041, *E. coli* AW677) and CheZ (*E. coli* RP1616) mutant strains were also examined. These had population RCDs between 1000 and 1100°·s^{-1}. All strains exhibited a reduced response sensitivity requiring photorelease of >100 μM serine for strong response. Response times for CheB strains were normal (~0.15 s), whereas the CheZ strain had greatly increased response time to attractant stimulation (Fig. 10 *a*), as previously shown by iontophoretic data (Segall et al., 1982). The CheB mutants exhibited no measurable response to caged proton photorelease. In contrast, CheZ responded (Fig. 10 *b*) with rapidity comparable with or greater than wild-type bacteria.

Inverse motility mutants (*S. typhimurium* ST120, ST124, and ST134 (Khan et al., 1978)) were also studied. Responses of all three strains to caged ligand photorelease were similar. No measurable increase in the population fraction of inverse swimming cells was observed upon caged proton photorelease. As observed with Che mutants, there was a marked reduction in response to serine photorelease. Photorelease of ~1 mM serine was required for a saturation (Fig. 10 *c*) and 20 μM serine for a detectible (Fig. 10 *d*) response. SPD, rather than RCD, provided the more sensitive measure of responses such as shown in Fig. 10 *d* where the bacteria remained tumbly but increased speed, presumably due to transition of individual flagellar filaments from curly to normal waveform, greater thrust resulting from the increased pitch (Khan et al., 1978). Response times were only modestly sensitive to stimulus strength and comparable with wild-type responses, indicating that filament transition mechanics did not affect response times.

A proportional relationship between stimulus strength and motor CW/CCW rotation ratio is indicated by all of these data. Such a relationship would result if the CW rotation state was obtained by binding a signal (S) to the motor in its CCW rotation state and if intracellular concentration of S varied with ligand (L) over the range studied; so that, $L^x \propto (xL) \cdot (R)/(R) \propto S^y \propto (yS) \cdot (\text{Motor}_{cw})/(\text{Motor}_{ccw}) = t_{cw}/t_{ccw}$; where R is receptor, t_{cw} is mean clockwise interval, t_{ccw} is mean counterclockwise interval, and x and y are (L)-(R) and (S)-Motor stoichiometry, respectively.

DISCUSSION

Macnab and Koshland (1972) first proposed that chemotactic response and adaptation may result from simultaneous activation of fast and slow catalytic processes controlling generation and decay of signal. This paradigm has provided a starting point for mechanistic analysis. It has been germane to considerations of sensory processing in more complex systems, e.g., hormonal responses (Li and Goldbeter, 1989) and neuronal guidance (Baier and Bonhoeffer, 1992), and has been used to establish interconnections between signal processing, amplification, and adaptation (Koshland et al., 1982; Kuo and Koshland, 1989). Quantitative models have been proposed that, in

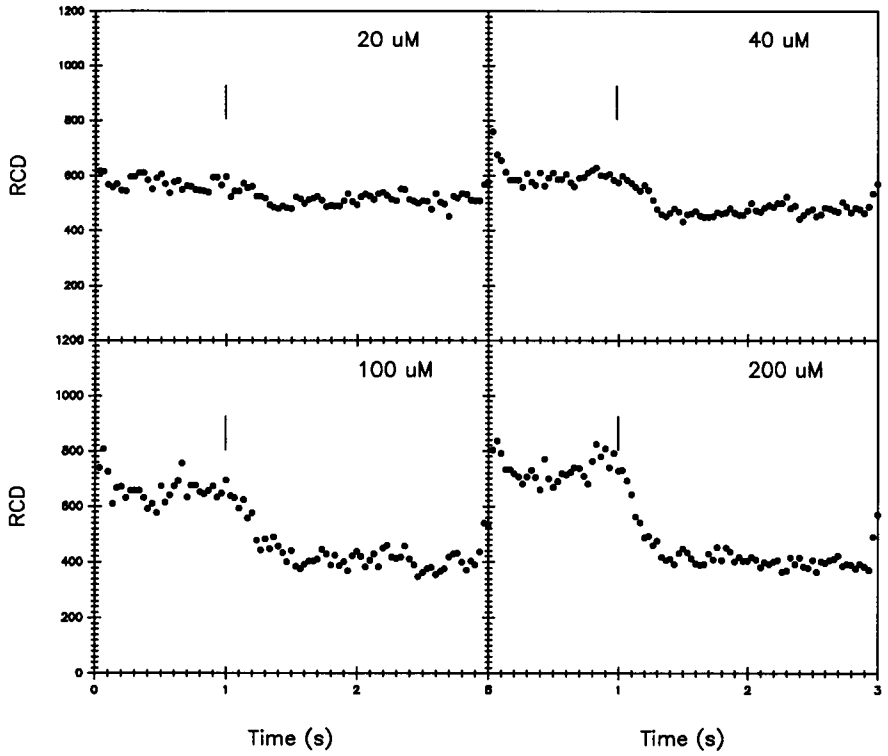

FIGURE 9 Excitation responses of an *E. coli* CheR-CheB mutant. RP2859 was the CheR-CheB strain used. Serine concentrations photoreleased are denoted on top right of each panel. Each panel represents more than 1000 motile paths. Vertical bars mark flashes. Response times and baseline RCD values were determined as detailed in Fig. 8. Saturation response time was 0.13 ± 0.02 s (200 μM serine).

principle, account for features such as exact adaptation (e.g., Knox et al., 1986). Physiological measurements have indicated that bacteria make weighted temporal comparisons (Segall et al., 1982) and have been interpreted in terms of models involving changes in receptor occupancy (Berg and Tedesco, 1975; Block et al., 1983; Spudich and Koshland, 1975). Finally, explicit biochemical models have been postulated based on in vitro measurements (see Introduction).

The status of biochemical knowledge regarding the chemotactic excitation signaling pathway is such that it has become feasible to attempt a quantitative evaluation of in vivo excitation behavior with in vitro biochemistry. The intracellular milieu affords combinatorial possibilities for interactions among the protein components of the chemotactic machinery and contains numerous ions (Tisa and Adler, 1992) and metabolites (Barak and Eisenbach, 1992b) that could alter protein biochemical reaction kinetics in vivo. Such considerations emphasize the need, as well as possible complexity, of such a task. It is clear a priori that a rapid assay is essential to limit and characterize possible mechanisms.

Response amplitudes and kinetics of wild-type and mutant bacteria to both attractant and repellent stimuli were determined in the present study. Response amplitude and motor rotation bias were correlated. Repellent responses saturated in the regime of rotation bias corresponding to incessant tumbling and did not attain the extreme bias corresponding to inverse swimming. This implies that maximal levels of the intracellular signal fail to drive flagellar motors into solely CW rotation in wild-type or *Che* mutant bacteria containing normal or fewer copy numbers of the Che proteins. Inverse motility has been observed only upon CheY overexpression (Wolfe and Berg, 1989) or motor mutation (Khan et al., 1978). This is consistent with ideas that CheY, or a form thereof, is the intracellular signal. Responses to attractants were observed, even at extreme CW bias. However, response sensitivity decreased as the shift away from normal bias became more severe, consistent with previous studies (see Block et al., 1982). With the exception of the CheZ mutant, responses to pH (repellent) jumps were immeasurable at high CW bias. The correlated reduction of response sensitivity for both attractants and repellents is most simply understood in terms of models in which motor response is determined by a common parameter whose intracellular concentration is the integrated output of both attractant and repellent signals. Elevated CW rotation values would reflect a higher intracellular concentration of this parameter and a stronger signal will be needed to bring about a fractional change in motor bias equivalent to that produced in wild-type bacteria. Stimuli effecting changes to restore wild-type levels (i.e., attractants) will evoke a greater response than stimuli of the opposite sign effecting changes toward even more extreme levels (i.e., repellents), consistent with observation. The reduced response sensitivity of CheR-CheB mutant strains remains unexplained.

There is no measurable latency in the population response. Saturation responses initiate within 0.033 s, the temporal resolution of the video data, after flash photorelease, in *V. alginolyticus* as well as *E. coli* and *S. typhimurium*. This is in marked contrast to the 0.25–0.7-s latencies observed during *Halobacterium halobium* phototactic responses (Sundberg et al., 1986). *H. halobium* is polarly multiflagellated and these response latencies may reflect specialized machinery for coordinated switching of the flagella. The re-

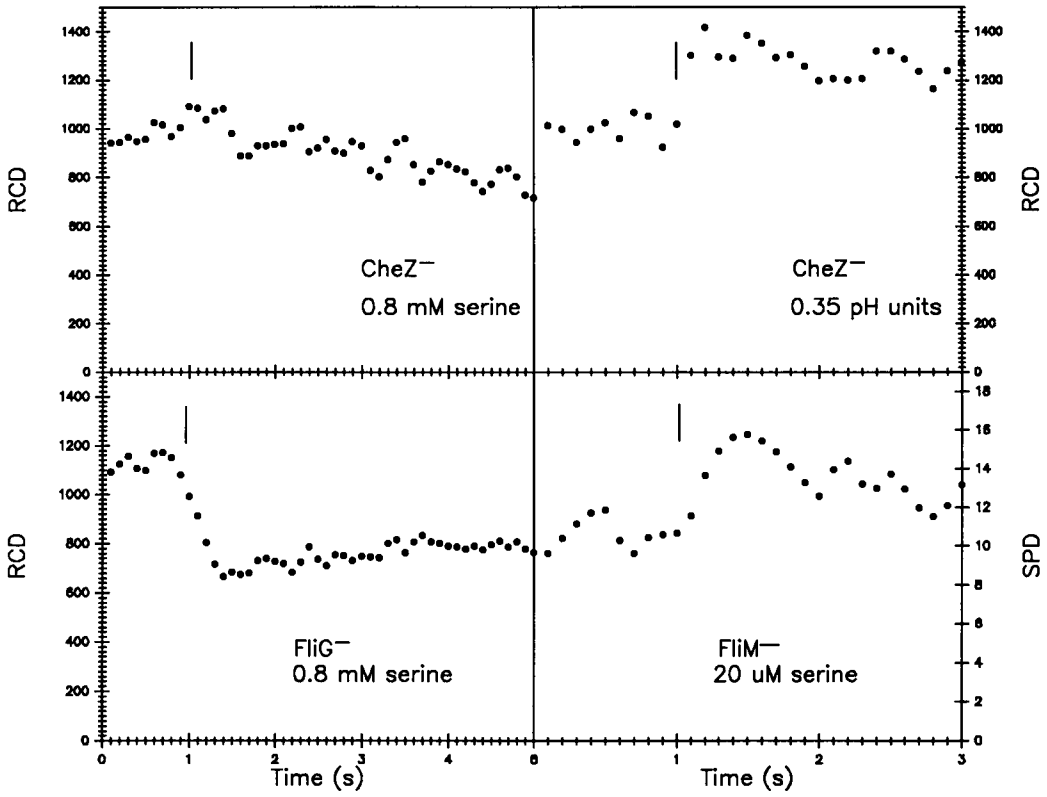

FIGURE 10 Excitation responses of *E. coli/S. typhimorion* mutants with CW motor bias. Mutant genotype and concentrations of photoreleased species are denoted on bottom right of each panel. Vertical bars mark flashes. Changes in RCD ($°\cdot s^{-1}$) and SPD ($\mu m\cdot s^{-1}$) are shown, as specified. The number of paths obtained per slide in these tumbly mutant bacteria was sharply reduced due to few bacteria being present at the top coverslip undersurface. From 100 to 500 paths were used for each panel and the data were smoothed by averaging over blocks of three frames each. CheZ RP1616 had maximal response times of ~5 s for serine, the response of the population shown eventually reaching minimum RCD values of $\sim 500°\cdot s^{-1}$; and < 0.1 s for protons. Response times of the inverse motility mutants ST134 and ST120 were 0.21 ± 0.02 and 0.18 ± 0.03 s to 0.8 and 0.02 mM serine, respectively.

sponse latencies (Segall et al., 1982) documented for responses of single *E. coli* motors probably reflect motor response times rather than motor deadtime before response initiation. The stimulus strength dependence of subsaturation response times suggests that these are limited in part by concentration-dependent reactions. Saturation response times, however, are relatively unaffected even at the extreme CW bias characteristic of the inverse motility phenotype.

How might the mutant response kinetics be rationalized in terms of current chemotaxis models? Insensitivity of saturation response times to motor bias, indicated by data obtained in this and previous studies (Block et al., 1982), simplifies identification of kinetically limiting components. The present study confirms that CheZ mutants process CCW signals slowly (Block et al., 1982; Segall et al., 1982, 1986), with a response time comparable with the spontaneous decay half-time of ~6 s determined in vitro (Hess et al., 1988) and, further, shows that CW signal processing is unaffected in such strains. These data are consistent with biochemical evidence that CheZ catalyzes CheY dephosphorylation. Absence of CheZ would affect the decrease of intracellular CheY·phosphate levels upon inhibition of CheA autophosphorylation by attractant, but not the increase induced by repellent. Interestingly, the CheZ strain was also the only mutant studied in which a measurable response to caged proton photorelease was observed. CheZ may interact with CheY and/or flagellar motors to affect CheY-motor interactions or with receptor complexes to modulate CheA autophosphorylation. The extreme CW bias of the motor mutants studied indicates that the CW rotation state of motors in these strains is more energetically stable than the CCW state and/or that the motors bind CheY tightly. In either case, the expectation would be that CW-to-CCW switching times would be increased in the mutant motors. Nevertheless, CCW signal response times in these strains are near normal. This implies that CCW signal response times are controlled by signal generation and/or other mechanisms for CheY phosphate decay rather than motor switch reactions. If ligand-based control of CheA autophosphorylation partly limits rates of decay or build-up of intracellular CheY·phosphate pools, the modest attractant ligand concentration dependence is easily explained. Little can be said, at present, regarding CW signal processing due to both inadequate temporal resolution and limited data.

We have combined advances in flash photolysis of caged chemicals, and high speed video processing of moving cell images to develop a rapid assay for measurement of excitation times in swimming *E. coli/S.typhimurium*. The relationship between signal processing kinetics and signal amplification is central to understanding of the sensory

response. Its elucidation through rapid screening of the available excitation pathway mutations is now feasible. The initial behavioral observations indicate future developments. Responses to repellents are distinct from responses to attractants in being more rapid and CheZ independent. Caged proton photolysis is sufficiently rapid for study of tumble signals, but the gain cannot be directly measured because changes in receptor protonation relevant for signal generation cannot be presently identified. Amino acid (e.g., leucine) repellents are thought to bind directly to Tsr (Eisenbach et al., 1990b). Synthesis of an appropriate caged amino acid should be possible given continuing developments in caging and rapid photorelease of amino acids (Corrie and Trentham, 1993). High speed cameras and high precision video instrumentation should enable more temporally resolved measurement of CW signal processing and identification of possible lesions that accelerate the process. The RCD computer measure of motile behavior should remain effective at higher digitization rates.

Mean population behavior has been documented in this study. The data are, however, stored as individual cell tracks. Analysis of cell-to-cell response variation should provide further information. Appropriate experimental geometries and repetitive flashes may be utilized to effect graded or impulsive application of stimuli for detailed analysis of the rotation of single tethered bacteria or flagellar filaments, as warranted. For example, the UV flash may be focused to effect photorelease from a spot for study of impulse responses. Programs for computerized analysis of single, tethered bacteria are available (Berg et al., 1987; Kuo and Koshland, 1989), and may be extended, upon appropriate modification, for analysis of whole fields of view. Tethered bacteria may mask (see Table 1) very brief intervals and pauses (Eisenbach et al., 1990a). Measurements of unloaded filament rotation (Kudo et al., 1990) may be more suitable for study of single motor behavior. Also, interpretation of complex stimulus-response behavior is qualified by assumptions, in particular that of system linearity, that are of uncertain validity. Nevertheless, it is apparent that the caged ligand-based computer assay for bacterial chemotactic excitation has significant potential for development, which when matched to advances in biochemical and structural knowledge, should ultimately reveal the chemical mechanism of the chemotactic response.

We thank Victoria Petri for assistance with the microscopy, Drs. H. C. Berg, J. Adler, R. M. Macnab, and J. S. Parkinson for bacterial strains, Dr. Jim Feeney for the H^1 NMR measurements of caged H^+ and 2-hydroxyphenyl phosphate, Dr. John E.T. Corrie for the protocol synthesis and characterization of the caged L-serine, and Dr. William R. Hand (Motion Analysis Inc.) for discussions on motion computer analysis.

This work was supported by grants GM38756 (to JLS and SK) and GM36936 (to SK) from the National Institutes of Health (NIH); by the Fogarty International Center of the National Institutes of Health; the Max Planck Society; and by NIH grant HLB 15835 to the Pennsylvania Muscle Institute. NMR spectra were recorded at the MRC Biomedical NMR Centre at the National Institute for Medical Research. Funds for purchase of the SPARC IPC computer and compatible EV Motion Analysis Software were obtained from shared instrumentation grant S10 RR06486 to JLS from the NIH. Funds for purchase of the Physik 201 MSC excimer laser were obtained from a grant from Boehringer Ingolheim Fonds.

REFERENCES

Adams, S. R., and Tsien, R. Y. 1993. Controlling cell chemistry with caged compounds. *Annu. Rev. Physiol.* 55:755–784.

Adler, J. 1973. A method for measuring chemotaxis and use of the method to determine optimum conditions for chemotaxis by *Escherichia coli*. *J. Gen. Microbiol.* 74:77–91.

Ames, P., and Parkinson, J. S. 1988. Transmembrane signaling by bacterial chemoreceptors: *E. coli* transducers with locked signal output. *Cell.* 55: 817–826.

Armitage, J. P., D. P. Josey, and D. G. Smith. 1977. A simple quantitative method for measuring chemotaxis and motility in bacteria. *J. Gen. Microbiol.* 102:199–202.

Baier, H., and Bonhoeffer, F. 1992. Axon guidance by gradients of a target-derived component. *Science.* 255:472–475.

Barak, R., and M. Eisenbach. 1992a. Correlation between phosphorylation of the chemotaxis protein CheY and its activity at the flagellar motor. *Biochemistry.* 31:1821–1826.

Barak, R., and M. Eisenbach. 1992b. Fumarate or a fumarate metabolite restores switching ability to rotating flagella of bacterial envelopes. *J. Bacteriol.* 174:643–645.

Berg, H. C. 1988. A physicist looks at bacterial chemotaxis. *Cold Spring Harbor Symp. Quant. Biol.* 53:1–9.

Berg, H. C., S. M. Block, M. P. Conley, A. R. Nathan, J. N. Power, and A. J. Wolfe. 1987. Computerized video analysis of tethered bacteria. *Rev. Sci. Instrum.* 58:418–423.

Berg, H. C., and D. A. Brown. 1972. Chemotaxis in *Escherichia coli* analysed by three-dimensional tracking. *Nature.* 239:500–504.

Berg, H. C., and P. M. Tedesco. 1975. Transient response to chemotactic stimuli in *Escherichia coli*. *Proc. Natl. Acad. Sci. USA.* 72:3235–3239.

Berg, H. C., and L. Turner. 1990. Chemotaxis of bacteria in glass capillary arrays. *Biophys. J.* 58:919–930.

Block, S. M., Segall, J. E., and H. C. Berg. 1982. Impulse responses in bacterial chemotaxis. *Cell.* 31:215–226.

Block, S. M., Segall, J. E., and H. C. Berg. 1983. Adaptation kinetics in bacterial chemotaxis. *J. Bacteriol.* 154:312–313.

Borkovich, K. A., and M. I. Simon. 1992. Attenuation of sensory receptor signaling by covalent modification. *Proc. Natl. Acad. Sci. USA.* 89: 6756–6761.

Bourret, R. B., Hess, J. F., and M. I. Simon. 1990. Conserved asparate residues and phosphorylation in signal transduction by the chemotaxis protein CheY. *Proc. Natl. Acad. Sci. USA.* 87:41–45.

Bourret, R. B., A. Borkovich, and M. I. Simon. 1991. Signal transduction pathways involving protein phosphorylation in prokaryotes. *Annu. Rev. Biochem.* 60:401–441.

Bourret, R. B., S. K. Drake, S. A. Chervitz, M. I. Simon, and J. J. Falke. 1993. Activation of the phospho-signaling protein, CheY. Analysis of activated mutants by ^{19}F-NMR and protein engineering. *J. Biol. Chem.* 268:13089–13096.

Clarke, S., and D. E. Koshland, Jr. 1979. Membrane receptors for aspartate and serine in bacterial chemotaxis. *J. Biol. Chem.* 254:9695–9702.

Corrie, J. E. T., and D. R. Trentham. 1993. Caged nucleotides and neurotransmitters. *In* Bioorganic Photochemistry. Vol. 2. H. Morrison, editor. John Wiley & Sons, Inc., New York. pp. 243–305.

Corrie, J. E. T., A. DeSantis, Y. Katayama, K. Khodakhah, J. B. Messenger, D. C. Ogden, and D. R. Trentham. 1993. Postsynaptic activation at the squid giant synapse by photolytic release of L-glutamate from a "caged" L-glutamate. *J. Physiol.* 465:1–8.

Dahlquist, F. W. P., P. Lovely, and D. E. Koshland, Jr. 1972. Quantitative analysis of bacterial migration in chemotaxis. *Nature.* 236:120–123.

Eisenbach, M., A. Wolf, M. Welch, S. R. Caplan, I. R. Lapidus, R. M. Macnab, H. Aloni, and O. Asher. 1990a. Pausing, switching and speed fluctuation of the bacterial flagellar motor and their relation to motility and chemotaxis. *J. Mol. Biol.* 211:551–563.

Eisenbach, M., C. Constantinou, H. Aloni, and M. Shinitzky. 1990b. Repellents for *Escherichia coli* operate neither by changing membrane fluidity nor being sensed by periplasmic receptors during chemotaxis.

J. Bacteriol. 172:5218–5224.

Gegner, J. A., D. R. Graham, A. F. Roth, and F. W. Dahlquist, 1992. Assembly of an MCP receptor, CheW, and kinase CheA complex in the bacterial chemotaxis signal transduction pathway. *Cell.* 70:975–982.

Ho, C. H., and J. M. Sturtevant. 1962. The kinetics of the hydration of carbon dioxide at 25°C. *J. Biol. Chem.* 238:3499–3501.

Hess, J. F., K. Oosawa, N. Kaplan, and M. I. Simon. 1988. Phosphorylation of three proteins in the signaling pathway of bacterial chemotaxis. *Cell.* 53:79–87.

Inoue, S. 1986. Video Microscopy. Plenum Press, New York.

Irie, M. 1983. Light-induced reversible pH change. *J. Am. Chem. Soc.* 105: 2078–2079.

Irikura, V. M., M. Kihara, S. Yamaguchi, H. Sockett, and R. M. Macnab. 1993. *Salmonella typhimurium fliG* and *fliN* mutations causing defects in assembly, rotation and switching of the flagellar motor. *J. Bacteriol.* 175: 802–810.

Janka, K., and J. Reichert. 1987. Proton concentration jumps and generation of transmembrane pH gradients by photolysis of 4-formyl-6-methoxy-3-nitrophenoxyacetic acid. *Biochim. Biophys. Acta.* 905:409–416.

Kaplan, J. A., B. Forbush. III, and J. F. Hoffman. 1978. Rapid photolytic release of adenosine 5′-triphosphate from a protected analogue: utilization by the Na:K pump of human red blood cell ghosts. *Biochemistry.* 17:1929–1935.

Khan, S., Macnab, R. M., DeFranco, A. L., and D. E. Koshland, Jr. 1978. Inversion of a behavioral response in bacterial chemotaxis: explanation at a molecular level. *Proc. Natl. Acad. Sci. USA.* 75:4150–4154.

Khan, S., and R. M Macnab. 1980. The steady-state counterclockwise-clockwise ratio of bacterial flagellar motors is regulated by protonmotive force. *J. Mol. Biol.* 138:563–599.

Khan, S., M. Meister, and H. C. Berg. 1985. Constraints on flagellar rotation. *J. Mol. Biol.* 184:645–656.

Khan, S., M. Dapice, and I. Humayun. 1990. Energy transduction in the bacterial flagellar motor: Effects of load and pH. *Biophys. J.* 57:779–796.

Khan, S., K. Amoyaw, J. L. Spudich, G. P. Reid, and D. R. Trentham. 1992. Bacterial chemoreceptor signalling probed by flash photorelease of a caged serine. *Biophys. J.* 62:67–68.

Kihara, M., and R. M. Macnab. 1981. Cytoplasmic pH mediates pH taxis and weak-acid repellent taxis of bacteria. *J. Bacteriol.* 145:1209–1221.

Knox, B. E., P. N. Devreotes, A. Goldbeter, and L. E. Segel. 1986. A molecular mechanism for sensory adaptation based on ligand-induced receptor modification. *Proc. Natl. Acad. Sci. USA.* 83:2345–2349.

Koshland, D. E. Jr., A. Goldbeter, and J. Stock. 1982. Amplification and adaptation in regulatory and sensory systems. *Science.* 217:220–225.

Kudo, S., Y. Magariyama, and S-I. Aizawa. 1990. Abrupt changes in flagellar rotation observed by laser dark-field microscopy. *Nature.* 346: 677–680.

Kuo, S. C., and D. E. Koshland, Jr. 1989. Multiple kinetic states for the flagellar motor switch. *J. Bacteriol.* 171:6279–6287.

Li, Y-X., and A. Goldbeter. 1989. Frequency specificity in intercellular communication. Influence of patterns of periodic signaling on target cell responsiveness. *Biophys. J.* 55:125–155.

Liu, J-Z., M. Dapice, and S. Khan. 1990. Ion selectivity of the *Vibrio alginolyticus* flagellar motor. *J. Bacteriol.* 172:5336–5244.

Lukat, G. S., B. H. Lee, J. M. Mottonen, A. M. Stock, and J. B. Stock. 1991. Roles of the highly conserved aspartate and lysine residues in the response regulator of bacterial chemotaxis. *J. Biol. Chem.* 266:8348–8354.

Macnab, R. M. 1987. Motility and chemotaxis. *In E. coli* and *S. typhimurium*: Cellular and Molecular Biology. Niedhardt et al., editors. ASM Publications, Washington, DC. 732–759.

Macnab, R. M., and D. E. Koshland, Jr. 1972. The gradient-sensing mechanism in bacterial chemotaxis. *Proc. Natl. Acad. Sci. USA.* 69:2509–2512.

Macnab, R. M., and D. E. Koshland, Jr. 1974. Bacterial motility and chemotaxis: light induced tumbling response and visualization of individual flagella. *J. Mol. Biol.* 84:399–406.

Marwan, W., and D. Oesterhelt. 1990. Quantitation of photochromism of sensory rhodopsin-I by computerized tracking of *Halobacterium halobium* cells. *J. Mol. Biol.* 215:277–285.

McCray, J. A., and D. R. Trentham. 1989. Properties and uses of photoreactive caged compounds. *Annu. Rev. Biophys. Biophys. Chem.* 18: 239–270.

Meister, M., G. Lowe, and H. C. Berg. 1987. The proton flux through the bacterial flagellar motor. *Cell.* 49:643–650.

Oosawa, K., J. F. Hess, and M. I. Simon. 1988. Mutants defective in bacterial chemotaxis show modified protein phosphorylation. *Cell.* 53:89–96.

Parkinson, J. S. 1978. Complementation analysis and deletion mapping of *Escherichia coli* mutants defective in chemotaxis. *J. Bacteriol.* 135:45–53.

Parkinson, J. S., and E. C. Kofoid. 1992. Communication modules in bacterial signaling proteins. *Annu. Rev. Genet.* 26:71–112.

Patchornik, A., B. Amit, and R. B. Woodward. 1970. Photosensitive protecting groups. *J. Am. Chem Soc.* 92:6333–6335.

Poole, P. S., D. R. Sinclair, and J. P. Armitage. 1988. Real time computer tracking of free-swimming and tethered rotating cells. *Anal. Biochem.* 175:52–58.

Roman, S. J., M. Meyers, K. Volz, and P. Matsumura. 1992. A chemotactic signaling surface on CheY defined by suppressors of flagellar switch mutations. *J. Bacteriol.* 174:6247–6255.

Repaske, D. R., and J. Adler. 1981. Change in intracellular pH of *Escherichia coli* mediates the chemotactic response to certain attractants and repellents. *J. Bacteriol.* 145:1196–1208.

Sager, B. M., J. J. Sekelsky, P. Matsumura, and J. Adler. 1988. Use of a computer to assay motility in bacteria. *Anal. Biochem.* 173:271–277.

Segall, J. E., M. D. Manson, and H. C. Berg. 1982. Signal processing times in bacterial chemotaxis. *Nature.* 296:855–857.

Segall, J. E., S. M. Block, and H. C. Berg. 1986. Temporal comparisons in bacterial chemotaxis. *Proc. Natl. Acad. Sci. USA.* 83:8987–8991.

Shimada, K., and H. C. Berg. 1987. Response of the flagellar rotary motor to abrupt changes in extracellular pH. *J. Mol. Biol.* 193:585–589.

Slonczewski, J. L., R. M. Macnab, J. R. Alger,, and A. M. Castle. 1982. Effects of pH and repellent tactic stimuli on protein methylation levels in *Escherichia coli. J. Bacteriol.* 152:384–399.

Sockett, E., S. Yamaguchi, M. Kihara, V. M. Irikura, and R. M. Macnab. 1992. Molecular analysis of the flagellar switch protein FliM of *Salmonella typhimurium. J. Bacteriol.* 174:793–806.

Springer, M. S., M. F. Goy, and J. Adler. 1979. Protein methylation in behavioral control mechanisms and in signal transduction. *Nature.* 280: 279–284.

Spudich, J. L., and D. E. Koshland, Jr. 1975. Quantitation of the sensory response in bacterial chemotaxis. *Proc. Natl. Acad. Sci. USA.* 72: 710–713.

Stock, A., and J. B. Stock. 1987. What is the role of protein methylation in bacterial chemotaxis. *Trends. Biochem. Sci.* 12:371–375.

Stock, J. B., Lukat, G. S., and A. M. Stock. 1991. Bacterial chemotaxis and the molecular logic of intracellular signal transduction networks. *Annu. Rev. Biophys. Biophys. Chem.* 20:109–136.

Sundberg, S. A., M. Alam, and J. L. Spudich. 1986. Excitation signal processing times in *Halobacterium halobium* phototaxis. *Biophys. J.* 50: 895–900.

Tisa, L. S., and J. Adler. 1992. Calcium ions are involved in *Escherichia coli* chemotaxis. *Proc. Natl. Acad. Sci. USA.* 89:11804–11808.

Tisa, L. S., B. M. Olivera, and J. Adler. 1993. Inhibition of *Escherichia coli* chemotaxis by ω-conotoxin, a calcium ion channel blocker. *J. Bacteriol.* 175:1235–1238.

Vary, P. S., and B. A. D. Stocker. 1973. Nonsense motility mutants in *Salmonella typhimurium. Genetics.* 73:229–245.

Walker, J. W., G. P. Reid, J. A. McCray, and D. R. Trentham. 1988. Photolabile 1-(2-nitrophenyl) ethyl phosphate esters of adenine analogues. Synthesis and mechanism of photolysis. *J. Am. Chem. Soc.* 110: 7170–7177.

Wang, T. T., S. H. Bishop, and A. Himoe. 1972. Detection of carbamate as a product of the carbamate catalyzed reaction by stopped-flow spectrophotometry. *J. Biol. Chem.* 247:4437–4439.

Weiss, R. M., and D. E. Koshland, Jr. 1988. Reversible receptor methylation is essential for normal chemotaxis of *Escherichia coli* in gradients of aspartic acid. *Proc. Natl. Acad. Sci. USA.* 85:83–87.

Wolfe, A. J., M. P. Conley, T. J. Kramer, and H. C. Berg. 1987. Reconstitution of signaling in bacterial chemotaxis. *J. Bacteriol.* 169: 1878–1885.

Wolfe, A. J., and H. C. Berg. 1989. Migration of bacteria in semisolid agar. *Proc. Natl. Acad. Sci. USA.* 86:6973–6977.